Effect of surfactants on morphology and textural parameters of silica nanoparticles derived from paddy husk and their efficient removal of methylene blue

Conference Paper · July 2021

DOI: 10.6084/m9.figshare.14904873

CITATIONS
2

READS
51

4 authors, including:

Himasha Gunathilaka
Sri Lanka Institute of Information Technology
3 PUBLICATIONS **2** CITATIONS
SEE PROFILE

Charitha Jayaruk Thambiliyagodage
Sri Lanka Institute of Information Technology, Malabe
32 PUBLICATIONS **117** CITATIONS
SEE PROFILE

Leshan Usgodaarachchi
Sri Lanka Institute of Information Technology
16 PUBLICATIONS **20** CITATIONS
SEE PROFILE

Effect of surfactants on morphology and textural parameters of silica nanoparticles derived from paddy husk and their efficient removal of methylene blue

Himasha Gunathilaka
School of Science and Education, Faculty of Humanities and Sciences,
Sri Lanka Institute of Information Technology,
Malabe, Colombo, Sri Lanka
himasha.g@sliit.lk

Charitha Thambiliyagodage
School of Science and Education, Faculty of Humanities and Sciences,
Sri Lanka Institute of Information Technology,
Malabe, Colombo, Sri Lanka
charitha.t@sliit.lk

Leshan Usgodaarchchi
Department of Materials Engineering, Faculty of Engineering,
Sri Lanka Institute of Information Technology,
Malabe, Colombo, Sri Lanka
leshan.u@sliit.lk

Sajeevan Angappan
Department of Materials Engineering, Faculty of Engineering,
Sri Lanka Institute of Information Technology,
Malabe, Colombo, Sri Lanka
sajeevanangappan@gmail.com

Abstract

Effective removal of textile dyes is important in environmental remediation especially for decontamination of wastewater. Herein, we report the synthesis of mesoporous silica nanoparticles (MSNs) from paddy husk with varying concentrations of surfactants, Cetyltrimethylammonium bromide (CTAB), and Polyethyleneglycol (PEG) by sol-gel synthesis method. Ratios of the surfactants CTAB: PEG were varied as 2:0 (MSN1),1:1 (MSN2), 0:2 (MSN3). MSNs were characterized by scanning electron microscope (SEM), Brunauer-Emmett-Teller surface area analyzer (BET), Thermogravimetric analyzer (TGA), and X-ray diffractometer. According to the SEM images, MSNs of all the combinations were aggregated with spherical and irregular shaped nanoparticles. MSNs synthesized with a 1:1 surfactant ratio showed more spherical nanoparticles. BET surface areas of MSN1, MSN2, and MSN3 are 468.35, 95.94, 177.46 m2/g, respectively. TGA curve indicated that desorption of the physisorbed water was completed at 125 °C. The effect of dye removal by the MSNs was studied on the adsorption of methylene blue (MB). Effect of dye concentration (5-30 mg/l), adsorbent dosage (5-20 mg), pH of the medium (2-10), ionic strength of the medium (0-6g/l NaCl), presence of a heavy metal (Pb2+- 0-500 mg/l) and temperature (25-55 °C) on MB adsorption was studied. At all the varied parameters, the adsorption efficiency of MB varied as MSN1> MSN3> MSN2, being similar to the trend of the surface area. The percentage of MB adsorption decreased with increasing MB concentration while it increased with increasing adsorbent dosage. The highest efficiency of MB adsorption was obtained at pH 10 and it decreased with increasing ionic strength and increasing concentration of heavy metal ions. The maximum percentage of MB adsorption resulted at 55 °C. Therefore, it can be concluded that the MSNs synthesized using only CTAB as the surfactant is an effective adsorbent in removing textile dyes from wastewater.

Keywords: Silica nanoparticles, Cetyltrimethylammonium bromide, Polyethyleneglycol, Methylene blue

I. INTRODUCTION

Pollutants are being released into the water reservoirs causing serious problems. Pollutants such as heavy metals, pesticides, fertilizers, hydrocarbons, biphenyls, detergents, oils, greases, pharmaceuticals etc.[1], [2] are released due to rapid industrialization. Among them, the release of dye molecules has critically impacted aquatic ecosystems as well as human health by causing allergies, neurological disorders, hypertension, cardiovascular diseases, and pulmonary diseases once absorbed through various pathways [3]–[5]. Dyes that are not readily biodegradable are released to water reservoirs by the runoffs from various industries such as textile, pharmaceutical, paper, plastic, food, pulp, etc. One of the main sources of dye waste is the textile industry. Many methods including Adsorption[6], coagulation/flocculation [7], Ion exchange [8], electrochemical processes [9], advanced oxidation processes [10], and bacterial biodegradation [11] have used to remove the dyes from wastewater. Adsorption is a promising wastewater treatment method as it could be applied to remove almost all the pollutants, and the method is

IEECP'21, July 29-30, 2021, Silicon Valley, San Francisco, CA – USA

DOI : *https://dx.doi.org/10.6084/m9.figshare.14904873*

inexpensive and easy to operate. In general, adsorption is the process where the substances are accumulated at a surface or an interface. Activated carbon (AC) is widely used to remove heavy metal ions and organic pollutants due to the high surface area resulted from the large micropore and mesopore volumes.[12], [13] In addition to AC adsorbents like carbon nanotubes,[14] zeolite,[15] sawdust,[16] seed shells,[17] maghemite nanoparticles,[18] clay material,[19] etc. have been used for wastewater purification. However, the blockage of micropores of activated carbon by macro dye molecules makes it more difficult for large dye molecules to diffuse into the internal pore structure of activated carbon, limiting its applicability [20]. Mesoporous silica is a porous material that has been used as an absorbent due to its unique surface and pore properties such as high surface area and high pore volumes [21]. In this study, we report the synthesis of mesoporous silica nanoparticles (MSN) using paddy husk which is an agricultural waste product. MSNs have been synthesized by the sol-gel method by using CTAB and PEG as the surfactants. Synthesized MSNs were used to remove methylene blue from artificial wastewater is also studied.

II. Methodology

Paddy husk were washed with water to remove the impurities. They were treated in 2 M Sulfuric acid for 3 hours at 110 °C under refluxing conditions. Acid treated paddy husk were washed with an abundant volume of DI water until a neutral pH is achieved. They were heated in a muffle furnace at 600 °C for 5 hours. Obtained white colour silica was treated with 4M KOH for 5 hours at 80 °C. The obtained solution was filtered and surfactants (CTAB and/or PEG) were added to the filtrate as tabulated below in table 1. The mixture was stirred for 30 minutes and 0.5 M sulfuric acid was added dropwise till pH reached 4. Obtained gel was aged for 8 hours and was washed with DI water until the washings are negative for Cl^- ions. The precipitate was dried and calcined at 600 °C for 5 hours.

Table 1. Surfactant/s added for the synthesis

Sample	% CTAB	% PEG
MSN1	2	0
MSN2	2	2
MSN3	0	2

Effect of the pH (2-10), dye concentration (5-30 mg/l), adsorbent dosage (5-20 mg), temperature (25-55 °C), ionic strength (NaCl, 2-6 g/l) and presence of heavy metal (Pb^{2+}, 100-500 mg/l) on adsorption of MB to the synthesized MSNs were determined. Generally, a known weight of MSN was shaken in a 25 ml of desired concentration of MB for one hour at room temperature.

III. RESULTS AND DISCUSSION

A. Morphological analysis

Morphology of the synthesized mesoporous MSNs (MSN1 – MSN3) was studied by SEM and TEM (Figure 1). SEM images show that spherical and irregular shaped nanoparticles are much aggregated and are in the range of 220 – 415 nm. MSNs of the MSN2 sample (Figure 1 (c)) are more spherical compared to the others. This observation is also supported by the TEM images where the TEM image of MSN1 (Figure 1 (e)) show more irregular shaped NPs, and the TEM image of MSN2 (Figure 1 (f)) show more spherical NPs. Therefore, it is evident that when CTAB and PEG are mixed in a 1:1 ratio more spherical NPs have resulted. Positively charged surfactant (CTAB) readily form interactions with the negatively charged silica. Neutral surfactant (PEG) forms hydrogen bonds with the hydroxyl groups on the silica surface [22]. Hence, by the action of both surfactants in equal proportions, NPs are located well apart from each other producing more spherical NPs. However, with other surfactant mixtures with different proportions more irregular shaped NPs have produced indicating that the NPs were not well separated and during calcination, at higher temperatures, they were aggregated due to Oswald ripening producing larger and irregular nanoparticles. However, the used surfactant concentrations are insufficient to produce well-dispersed uniform NPs.

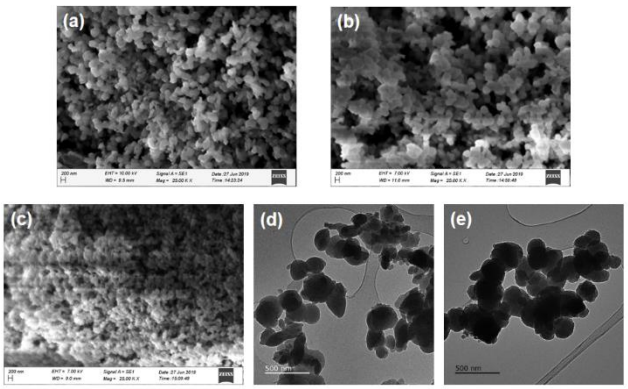

Figure 1. SEM images of (a) MSN1 (b) MSN2 (c) MSN3 TEM images of (d) MSN1 (e) MSN 2

B. FT-IR analysis

FT-IR spectra were acquired to study the bonding nature of the MSNs and effective surface functionalization by the surfactants (Figure 2). The bands at 1050 and 800 cm-1 is attributed to the Si-O-Si stretching and Si-O bending frequencies. The band at 460 cm-1 is assigned to Si-O out of plane deformation [23], [24]. The band at 1620 cm-1 corresponds to C=O vibration of carboxyl, lactonic and anhydride groups [25]. The peak at 2950 cm-1 is attributed to the C-H stretching frequency, indicating the presence of CH_2 group suggesting that the MSN surface has been functionalized by PEG and CTAB used for particle dispersion [26]. A broad band at 3400 cm-1 is assigned to the O-H stretching indicating the presence of H_2O as moisture [24].

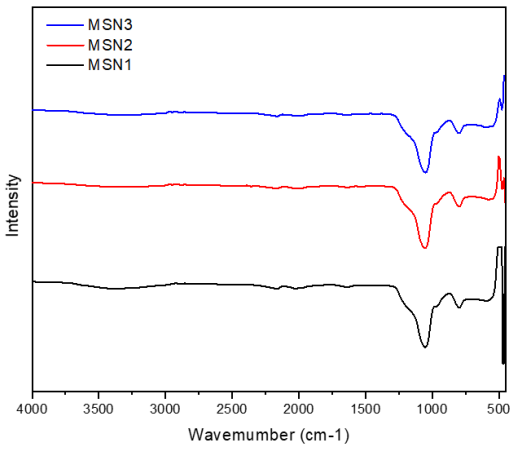

Figure 2. FT-IR spectra of the synthesized MSNs.

C. XRD analysis

XRD pattern (Figure 3) shows a broad peak centered at $2\theta = 21.5°$ indicating the amorphous nature of the synthesized MSNs. Further, any peaks correspond to crystalline silica were not present suggesting that during acid leaching of paddy husk metal ions

associated such as Ca, Mg, K, Fe, Mn have been leached out preventing the formation of crystalline silica. On the other hand, calcined temperature (550 °C) is insufficient to produce crystalline silica.

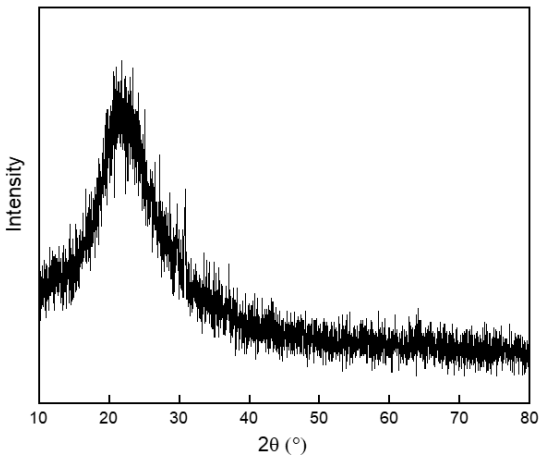

Figure 3. XRD pattern of MSN1

D. Surface area analysis

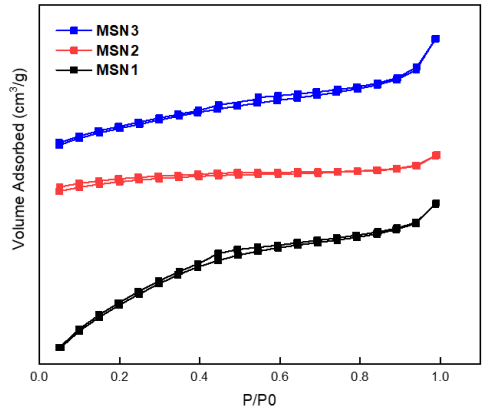

(a)

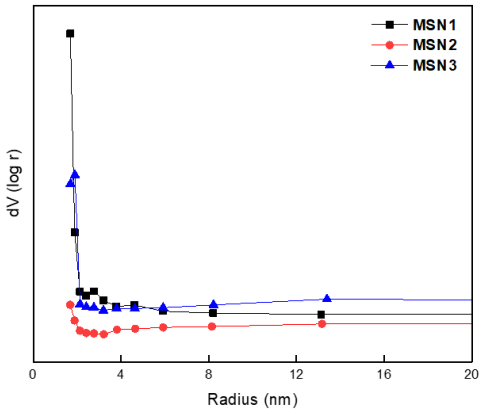

(b)

Figure 4. (a) BET isotherms (b) BJH Pore size distribution curves of MSNs

BET adsorption-desorption isotherms and BJH pore size distribution curves were collected to study the textural properties including surface area, total pore volume and average pore size. All three BET adsorption and desorption isotherms (Figure 4(a)) belong to the type V with H2 hysteresis loop indicating the presence of disordered mesopores where the distribution of pore size and shape is not well defined. BJH pore size distribution curves (Figure 4 (b)) also support this observation where the board pore size distributions have resulted. The surface area of the MSNs vary in the order of MSN1> MSN3> MSN2 of which the highest surface area (468.35 m2/g) was obtained in MSN1 and the least (95.94 m2/g) resulted in MSN2. The total pore volume of MSNs varied as MSN1> MSN3> MSN2 as tabulated in Table 1. Hence, it is evident that with equal proportions of the surfactants (MSN2) pore network has not been established properly resulting in low surface area and pore volumes. Surfactants exist as monomolecular at lower concentrations but at higher concentrations, they tend to form micelles to decrease the system entropy. Surfactants driven porous structure is determined by the concentration of the surfactant, length of the hydrophobic chain, hydrophilic head group, and the counter ion in the case of ionic surfactants. Here, in this study, two different surfactants (CTAB and PEG) with different properties were used. CTAB is a cationic surfactant and PEG is a neutral surfactant. CTAB interacts with silica via Coulombic attractions and PEG interacts via Hydrogen bonds with silica surface hydroxyl groups. CTAB has a hydrophilic group at the end of the CTAB chain. This end interacts with the silica surface. CTAB chain is long and CTAB hydrophobic chains repel each other separating MSNs effectively. At calcination, CTAB molecules removed creating a well-established porosity and hence a high surface area as obtained for MSN1 in this study. Each hydrophilic group of PEG lies in between two -CH2- groups. This makes the PEG molecules diffuse faster and form the directional alignment on the surface rather than forming a micelle structure. Adsorbed PEG molecules on the silica surface could hinder the growth of the particles through steric hindrance or could lead to the formation and large silica clusters. Here as PEG 6000 was used agglomeration effect has taken place rather than the steric hindrance effect due to high molecular weight. This has led to low surface area in MSN3 compared to MSN1. CTAB on MSNs is not closely arranged as they repel each other. PEG molecules easily get inserted into the loosely adsorbed CTAB layers due to the hydrophobic effect and dipole –ion interactions that may have generated between two surfactants. Hence, the repulsive forces between the same charged particles are reduced and the density of the hydrophobic chains are increased. Further, oxygen entities of the PEG could get positively charged due to the interactions with H^+ in water. Therefore, this creates a repulsive force with the CTAB molecules and hence as a consequence surfactant mixtures disperse the MSNs well forming more spherical NPs as shown in SEM and TEM images [27]. However, the coexistence of two surfactants affects the development of the porous structure leading to lower surface area (MSN2) compared to the MSNs where only one surfactant was used (MSN1 and MSN3).

Table 2. Textural parameters of the synthesized MSNs

Sample	BET Surface area (m^2/g)	Total pore volume (cc/g)	Average pore size (nm)
MSN1	468.35	0.332	1.42
MSN2	95.94	0.076	1.60
MSN3	177.46	0.189	2.13

E. Effect of different parameters

Effect of pH, dye concentration, adsorbent dosage, ionic strength, presence of a heavy metal (Pb^{2+}), and temperature on percentage removal of MB was studied (Figure 5). It could be seen that the highest % removal was obtained by MSN1, while the least by MSN2 for all the parameters tested. The obtained trend of data variation is consistent with the pattern of surface area and total pore volume

variation resulted in surface area analysis. MSN1 has the highest surface area and total pore volume while MSN2 has the least. Hence, MSN1 has a high number of active sites for adsorption compared to MSN2 and MSN3 and the activity of MSN3 is greater than that of MSN2 due to the same reason. The highest percentage removal of MB was obtained at pH 10 and the % removal increased with increasing pH. At pH 2 only 13.55% of MB was removed and 80.94% was removed at pH 10 by MSN1. MSN2 and MSN3 also show the same trend with varying pH. MB molecules are positively charged and has a high affinity to the negatively charged silica surfaces. However, at low pH values H^+ ions also readily adsorb to the silica surface. Therefore, at low pH values, there is a competition between H^+ and MB molecules. Adsorption of H^+ ions is high compared to the MB as the H^+ readily adsorb due to their small size and occupy the adsorption surface and due to the steric hindrance adsorption of MB molecules is less. However, at high pH values adsorption of MB is high because the abundant positively charged species is MB.

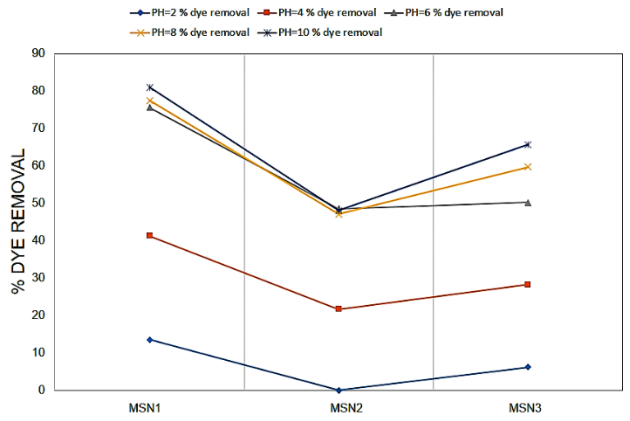

Figure 5. Effect of pH on dye removal by MSNs

Effect of dye concentration on % removal was determined in a concentration range of 5-30 mg/l (Figure 6). MSN1 was capable of removing 73.64% of 5 ppm MB in one hour while only 32.82% was removed by when 30 mg/l of MB was used.% removal of MB decreased with increasing dye concentration by all synthesized MSN. As the weight of the adsorbent is constant, the number of adsorption sites is the factor that limits the adsorption. Therefore, at high dye concentrations though more dye molecules are present sufficient number of adsorption sites are not available for adsorption resulting in low % removals.

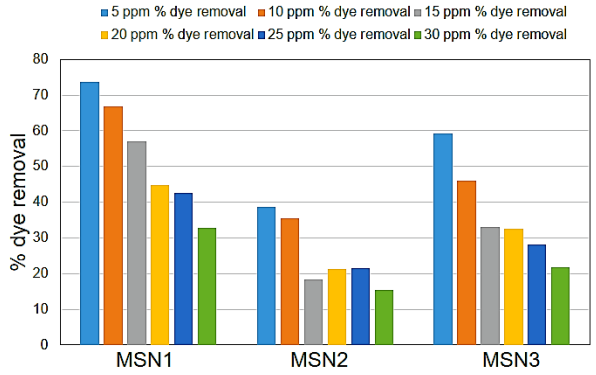

Figure 6. Effect of dye concentration on dye removal by MSNs

Adsorbent dosage was varied in the range of 5-20 mg to determine the effect of the weight of the adsorbent on the % removal of MB (Figure 7). The percentage removal of 86.47% was obtained by using 20 mg and only 57.14% removal was resulted with 5 mg of MSN1. With increasing, adsorbent dosage % removal of MB increased as high adsorbent weights of all three MSN due to the presence of more adsorption sites.

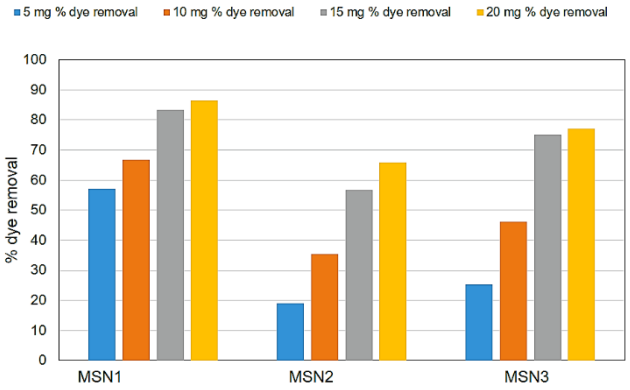

Figure 7. Effect of adsorbent dosage on dye removal by MSNs

The presence of ionic salts affects the adsorption of MB to silica surface where reduced adsorption was obtained with NaCl in the medium (Figure 8). Ionic salts interfere with the adsorption process in two mechanisms. According to the first mechanism, Na^+ compete with positively charged MB molecules to the adsorption sites resulting in low adsorption of MB due to the steric hindrance. The second mechanism explains that an increased ionic strength compress the double electric layer and lead to electrostatic repulsion of MB from the surface [28]–[30]. MSN1 has removed 66.80% of MB without added NaCl but with 6 g/l NaCl in the medium only 53.23 % of MB has been removed. Similarly, the % removal of MB has decreased with increasing NaCl concentration in all MSNs studied.

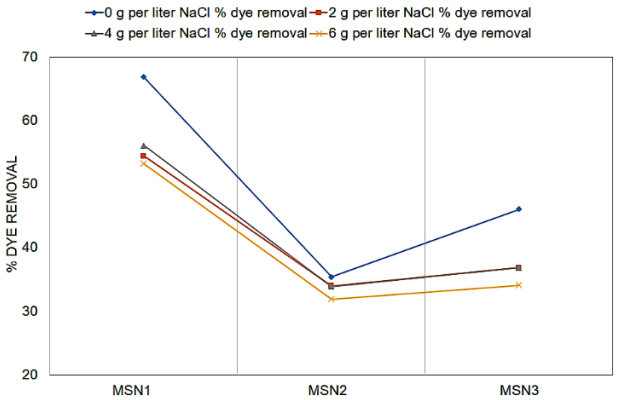

Figure 8. Effect of ionic strength on dye removal by MSNs

The effect of the presence of heavy metal on the removal of MB by MSN has been tested by using Pb^{2+} as the heavy metal ion (Figure 9). Positively charged metal ions and MB compete to the silica surface available and as Pb^{2+} are small in size compared to MB, more Pb^{2+} adsorb to the negatively charged silica surface and MB shows comparatively less adsorption due to the steric hindrance. The percentage of dye removal decreased with increasing Pb^{2+} concentration in all MSNs studied. The percentage removal of 66.80 % of MB was achieved by MSN1 in the absence of Pb^{2+}, with 100 mg/l Pb2+ in the medium 51.19 % MB was removed and 38.84% was removed in the presence of 500 mg/l Pb^{2+} in the medium.

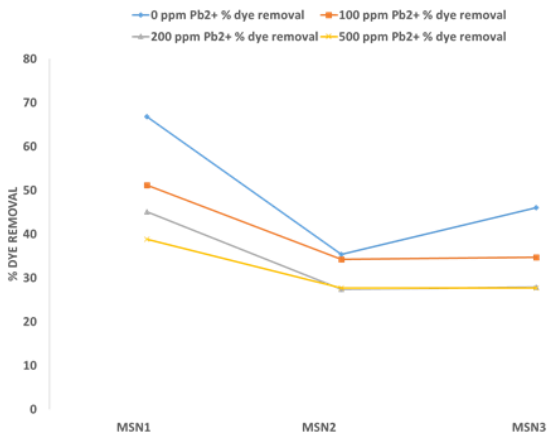

Figure 9. Effect of heavy metals on dye removal by MSNs

Adsorption of MB to silica is also affected by temperature. The effect of temperature was determined at different temperatures (25 - 55 °C) (Figure 10). MSN1 was capable of removing 60% of MB at 25 °C, while 74.52% of MB was removed at 55 °C. Percentage removal increased with increasing temperature in all the MSNs synthesized. Kinetic energy and the velocity of the dye molecules increase with increasing temperature. Therefore, the percentage of molecules with sufficient energy to reach the adsorbent surface at a given time is high at higher temperatures. This results in higher % removal of MB at high temperatures.

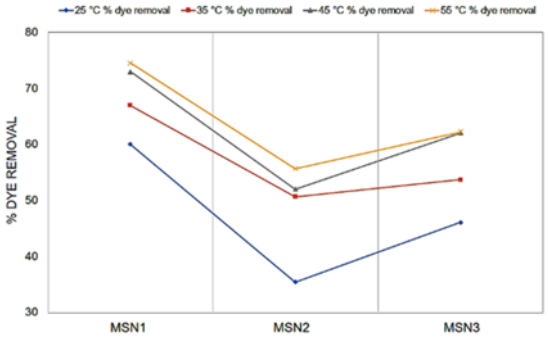

Figure 10. Effect of temperature on dye removal by MSNs

F. CONCLUSIONS

MSNs were successfully synthesized by the sol-gel method using paddy husk as the raw material using CTAB and/or PEG as the surfactants. Synthesized MSN were effective in removing MB. MSN1 showed the highest activity on removing MB followed by MSN3. MSN2 exhibited the least activity. Surface area and total pore volume were high in MSN1 followed by MSN3 and MSN2. Dye adsorption was maximum with 5 ppm MB, 20 mg of adsorbent, pH 10 and at 55 °C. The presence of NaCl and Pb2+ retarded the adsorption of MB.

IV. ACKNOWLEDGMENTS

Authors acknowledge Sri Lanka Institute of Information Technology for the financial support and Sri Lanka Institute of Nanotechnology for providing the instrument facilities.

V. REFERENCES

[1] "Low cost adsorbents for the removal of organic pollutants from wastewater," J. Environ. Manage., vol. 113, pp. 170–183, Dec. 2012, doi: 10.1016/J.JENVMAN.2012.08.028.

[2] M. Nageeb, "Adsorption Technique for the Removal of Organic Pollutants from Water and Wastewater," in Organic Pollutants - Monitoring, Risk and Treatment, InTech, 2013.

[3] H. M. Salem and A. A. Elfouly, "Minerals Reconnaissance at Saint Catherine Area, Southern Central Sinai, Egypt and their Environmental Impacts on Human Health."

[4] G. Bringmann and R. Kühn, "Comparison of the toxicity thresholds of water pollutants to bacteria, algae, and protozoa in the cell multiplication inhibition test," Water Res., vol. 14, no. 3, pp. 231–241, Jan. 1980, doi: 10.1016/0043-1354(80)90093-7.

[5] W. Guo, X. Liu, Z. Liu, and G. Li, "Pollution and potential ecological risk evaluation of heavy metals in the sediments around Dongjiang Harbor, Tianjin," in Procedia Environmental Sciences, Jan. 2010, vol. 2, pp. 729–736, doi: 10.1016/j.proenv.2010.10.084.

[6] M. T. Yagub, T. K. Sen, S. Afroze, and H. M. Ang, "Dye and its removal from aqueous solution by adsorption: A review," Advances in Colloid and Interface Science, vol. 209. Elsevier, pp. 172–184, Jul. 01, 2014, doi: 10.1016/j.cis.2014.04.002.

[7] S. Sadri Moghaddam, M. R. Alavi Moghaddam, and M. Arami, "Coagulation/flocculation process for dye removal using sludge from water treatment plant: Optimization through response surface methodology," J. Hazard. Mater., vol. 175, no. 1–3, pp. 651–657, Mar. 2010, doi: 10.1016/j.jhazmat.2009.10.058.

[8] S. Raghu and C. Ahmed Basha, "Chemical or electrochemical techniques, followed by ion exchange, for recycle of textile dye wastewater," J. Hazard. Mater., vol. 149, no. 2, pp. 324–330, Oct. 2007, doi: 10.1016/j.jhazmat.2007.03.087.

[9] C. A. Martínez-Huitle and E. Brillas, "Decontamination of wastewaters containing synthetic organic dyes by electrochemical methods: A general review," Applied Catalysis B: Environmental, vol. 87, no. 3–4. Elsevier, pp. 105–145, Apr. 2009, doi: 10.1016/j.apcatb.2008.09.017.

[10] S. H. S. Chan, T. Yeong Wu, J. C. Juan, and C. Y. Teh, "Recent developments of metal oxide semiconductors as photocatalysts in advanced oxidation processes (AOPs) for treatment of dye waste-water," J. Chem. Technol. Biotechnol., vol. 86, no. 9, pp. 1130–1158, Sep. 2011, doi: https://doi.org/10.1002/jctb.2636.

[11] A. Khalid, M. Arshad, and D. E. Crowley, "Biodegradation potential of pure and mixed bacterial cultures for removal of 4-nitroaniline from textile dye wastewater," Water Res., vol. 43, no. 4, pp. 1110–1116, Mar. 2009, doi: 10.1016/j.watres.2008.11.045.

[12] A. Jusoh, L. Su Shiung, N. Ali, and M. J. M. M. Noor, "A simulation study of the removal efficiency of granular activated carbon on cadmium and lead," Desalination, vol. 206, no. 1–3, pp. 9–16, Feb. 2007, doi: 10.1016/J.DESAL.2006.04.048.

[13] P. G. González and Y. B. Pliego-Cuervo, "Adsorption of Cd(II), Hg(II) and Zn(II) from aqueous solution using mesoporous activated carbon produced from Bambusa vulgaris striata," Chem. Eng. Res. Des., vol. 92, no. 11, pp. 2715–2724, Nov. 2014, doi: 10.1016/J.CHERD.2014.02.013.

[14] H. Wang, A. Zhou, F. Peng, H. Yu, and J. Yang, "Mechanism study on adsorption of acidified multiwalled carbon nanotubes to Pb(II)," J. Colloid Interface Sci., vol. 316, no. 2, pp. 277–283, Dec. 2007, doi: 10.1016/J.JCIS.2007.07.075.

[15] R. Apiratikul and P. Pavasant, "Sorption of Cu2+, Cd2+, and Pb2+ using modified zeolite from coal fly ash," Chem. Eng. J., vol. 144, no. 2, pp. 245–258, Oct. 2008, doi: 10.1016/j.cej.2008.01.038.

[16] F. Kaczala, M. Marques, and W. Hogland, "Lead and vanadium removal from a real industrial wastewater by gravitational settling/sedimentation and sorption onto Pinus sylvestris sawdust," Bioresour. Technol., vol. 100, no. 1, pp. 235–243, Jan. 2009, doi: 10.1016/J.BIORTECH.2008.05.055.

[17] O. S. Amuda, F. E. Adelowo, and M. O. Ologunde, "Kinetics and equilibrium studies of adsorption of chromium(VI) ion from industrial wastewater using Chrysophyllum albidum (Sapotaceae) seed shells," Colloids Surfaces B Biointerfaces, vol. 68, no. 2, pp. 184–192, Feb. 2009, doi: 10.1016/J.COLSURFB.2008.10.002.

[18] *,†,‡ Mélanie Auffan et al., "Enhanced Adsorption of Arsenic onto Maghemites Nanoparticles: As(III) as a Probe of the Surface Structure and Heterogeneity," 2008, doi: 10.1021/LA702998X.

[19] G. McKay, M. S. Otterburn, and J. A. Aga, "Fuller's earth and fired clay as adsorbents for dyestuffs," Water. Air. Soil Pollut., vol. 24, no. 3, pp. 307–322, Mar. 1985, doi: 10.1007/BF00161790.

[20] X. Zhuang, Y. Wan, C. Feng, Y. Shen, and D. Zhao, "Highly efficient adsorption of bulky dye molecules in wastewater on ordered mesoporous carbons," Chem. Mater., vol. 21, no. 4, pp. 706–716, Feb. 2009, doi: 10.1021/cm8028577.

[21] C. H. Huang, K. P. Chang, H. De Ou, Y. C. Chiang, and C. F. Wang, "Adsorption of cationic dyes onto mesoporous silica," Microporous Mesoporous Mater., vol. 141, no. 1–3, pp. 102–109, May 2011, doi: 10.1016/j.micromeso.2010.11.002.

[22] R. L. Derosa and J. A. Trapasso, "Poly(ethylene glycol) interactions with alumina and silica powders determined via DRIFT," J. Mater. Sci., vol. 37, no. 6, pp. 1079–1082, Mar. 2002, doi: 10.1023/A:1014328716329.

[23] C. J. Thambiliyagodage, V. Y. Cooray, I. N. Perera, and R. D. Wijesekera, "Eco-Friendly Porous Carbon Materials for Wastewater Treatment," in Lecture Notes in Civil Engineering, vol. 44, Springer, 2020, pp. 252–260.

[24] B. Shokri, M. A. Firouzjah, and S. I. Hosseini, "FTIR analysis of silicon dioxide thin film deposited by metal organic-based PECVD," in Proceedings of 19th international symposium on plasma chemistry society, 2009, vol. 2631, pp. 26–31.

[25] F.-N. Allouche, N. Yassaa, and H. Lounici, "Sorption of Methyl Orange from Aqueous Solution on Chitosan Biomass," Procedia Earth Planet. Sci., vol. 15, pp. 596–601, Jan. 2015, doi: 10.1016/j.proeps.2015.08.109.

[26] B. Lin and S. Zhou, "Poly(ethylene glycol)-grafted silica nanoparticles for highly hydrophilic acrylic-based polyurethane coatings," Prog. Org. Coatings, vol. 106, pp. 145–154, May 2017, doi: 10.1016/j.porgcoat.2017.02.008.

[27] D. Liu, L. Fang, and F. Cheng, "Bisurfactant-assisted preparation of amorphous silica from fly ash," Asia-Pacific J. Chem. Eng., vol. 11, no. 6, pp. 884–892, Nov. 2016, doi: 10.1002/apj.2022.

[28] P. Pimol, M. Khanidtha, and P. Prasert, "Influence of particle size and salinity on adsorption of basic dyes by agricultural waste: dried Seagrape (Caulerpa lentillifera)," J. Environ. Sci., vol. 20, no. 6, pp. 760–768, Jan. 2008, doi: 10.1016/S1001-0742(08)62124-5.

[29] C. H. Weng, Y. T. Lin, and T. W. Tzeng, "Removal of methylene blue from aqueous solution by adsorption onto pineapple leaf powder," J. Hazard. Mater., vol. 170, no. 1, pp. 417–424, Oct. 2009, doi: 10.1016/j.jhazmat.2009.04.080.

[30] C. E. de F. Silva, B. M. V. da Gama, A. H. da S. Gonçalves, J. A. Medeiros, and A. K. de S. Abud, "Basic-dye adsorption in albedo residue: Effect of pH, contact time, temperature, dye concentration, biomass dosage, rotation and ionic strength," J. King Saud Univ. - Eng. Sci., vol. 32, no. 6, pp. 351–359, Sep. 2020, doi: 10.1016/j.jksues.2019.04.006.